Fracture Mechanics of Concrete Structures
Proceedings FRAMCOS-3
AEDIFICATIO Publishers, D-79104 Freiburg, Germany

FAILURE OF CONCRETE UNDER UNIAXIAL COMPRESSION: AN OVERVIEW

J.G.M. van Mier
Faculty of Civil Engineering and Geosciences, Delft University of Technology, Delft, The Netherlands

Abstract
In the paper an overview of fracture of concrete subjected to uniaxial compression is given. Since the past few years, attention for compressive fracture has increased, in particular when it was found that localization of deformations occurs in uniaxial compression experiments on prisms with varying height. In addition an enormous dependency of post-peak behaviour on frictional constraint caused by some type of loading platens hampers the determination of a unique stress-strain curve for concrete under compression. This implies that fracture mechanics principles apply. The fracture process is complicated however because the amount of pre-critical crack growth is much larger than in tension, whereas frictional slip in cracks seems to contribute to the total compressive fracture energy as well. At this stage it is not clear which compressive stress-strain (or stress-displacement) diagram should be used for analyzing structures failing in compression.
Keywords: Uniaxial compression, softening, standard test, meso-level failure mechanism, localization, size effect, boundary constraint

1 Introduction
After the development of the Fictitious Crack Model by Hillerborg and co-workers (1976), there have been decades of increased interest in fracture

mechanics applied to concrete, in particular for tensile states of stress. As a result, the interest to study compressive failure has dwindled, but seems to catch on again in the past few years. Knowledge of the compressive stress-strain curve is important when it comes to assessing the rotational capacity of reinforced concrete beams. In many cases, when a non-linear finite element code is used, a complete constitutive law for concrete under multiaxial stress should be included. Many laws have been developed over the past years, from plasticity based theories, to plastic fracturing, endochronic, microplane model, and higher order continuum theories, see for example in Chen (1982) and Mühlhaus (1995). The finding that deformations localize in a narrow zone in (multiaxial) compression (in the brittle field, i.e. below the brittle-ductile transition, cf. Van Mier 1984) enforced a stop on the development of constitutive equations. Instead, the attention focused on modelling the (strain-) localization.

The fracture process of concrete under uniaxial and multiaxial compression (below the brittle to ductile transition) is a complicated three dimensional crack growth process. Obviously, many different mechanisms occur at the particle level - or meso-level - of the concrete. These fracturing processes, as well as frictional effects and micro-plasticity events lead to a macroscopic non-linear stress-strain behaviour. In the pre-peak part of the stress-strain curve, the energy dissipation from all these meso-level mechanisms is small compared to the total energy stored in the specimen, to allow for a continuum based approach. In the post-peak regime, however, specimen-machine interactions and geometrical effects become important, and the use of 'strain' as state variable becomes highly debatable. In Figure 1 a separation between pre-peak stress-strain behaviour and post-peak stress-deformation behaviour is shown.

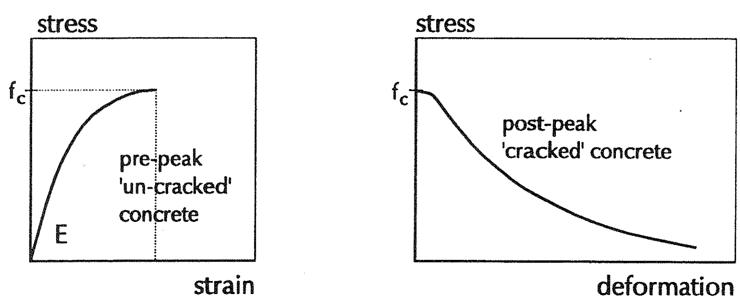

Fig 1. Pre-peak stress-strain curve (a) and post-peak stress-deformation curve (b) for concrete subjected to uniaxial compression, after Van Mier et al. (1997).

Note that the terms 'un-cracked' and 'cracked' in Figure 1 refer to the macrocracks that are visible to the naked eye. Interactions with the experimental environment occur when the size of the cracks is comparable to the characteristic size of the specimen. Thus, for cases where the post-peak behaviour is expected to play an important role on the behaviour of a (reinforced) concrete structure, complications arise. Hillerborg (1990) and Markeset (1993) were among the first to recognise the problem in assessing the rotational capacity of reinforced concrete structures. The assessment of rotational capacity was brought in the realm of fracture mechanics. In fact, Hillerborg proposed a model quite similar to the Fictitious Crack Model for tensile fracture. Although some progress has been made over the past two decades in the field of compressive fracture, it has to be seen whether a simplified fracture mechanics models is sufficient. Many details about the meso-level mechanisms remain to be solved. In this paper, a review of the mechanical behaviour of concrete under uniaxial compression will be presented. After a discussion of stiffness and pre-peak crack processes, the specimen-machine interactions that become important near and after the stress peak will be debated. The RILEM committee 148ssc has proposed a new test method for the measurement of the complete compressive stress-'strain' curve. Although a test recommendation has still to be written, some personal ideas about such a test will be included in this paper.

In the discussion, mechanisms occurring at the particle level of the concrete (meso-level) and at the macro-level (continuum assumption, which is true only if the size of the considered element is larger than 3-5 times the largest aggregate size in the material) will be considered. At the meso-level, the material is regarded as a particle stack by some researchers, whereas others normally depict the material as 'aggregates swimming in a matrix'. This latter view is popular because a planar section of concrete shows the material in this way. Obviously the three-dimensional structure is hard to identify from planar sections. In the discussion it will be attempted to regard the material as 3D and the fracturing as a three-dimensional process.

2 Pre-peak behaviour

In this section it is attempted to summarize a number of ideas that exist about the pre-peak fracturing of concrete at the meso- and macro-level. If the material is described at the macro-level, basically the non-linear behaviour must be incorporated in the constitutive equations. In that case the stress-deformation curve must be measured from a representative volume, which must be larger than a multiple of the largest aggregates in the mixture. For a better understanding of the non-linear macroscopic behaviour, however, a meso-level approach can be quite helpful, and may show the way to overcome difficulties that are apparent at the macro-level, in particular in the post-peak regime.

At the meso-level, the concrete can be regarded in two different ways (although perhaps other approaches may exist which are overlooked at the moment). The first and most popular meso-level model is shown in Figure 2a. Aggregates swim in a matrix of cement matrix (also containing small sand particles), and an interfacial transition zone encloses the larger aggregates. Normally it is assumed that the interfacial transition zone has a width of about 30 μm, and that it has a constant strength and stiffness over the entire volume. Recently, evidence has been presented that showed that the distribution of hydration products and porosity over the interface is quite non-uniform, and the view of a continuum interfacial transition zone must be doubted, see for example Diamond & Huang (1998). Following the second approach in Figure 2b, the structure of concrete is assumed to resemble that of a particle material like many soils. The differences are however that the size distribution of the particles deviates over 4 orders of magnitude, and cohesion exists between the different particles. Moreover, the particles are made of many different materials like cement, fillers and (natural) aggregates. Another complicating factor is that flocculation of cement particles may lead to local conglomerates of hardened cement paste particles.

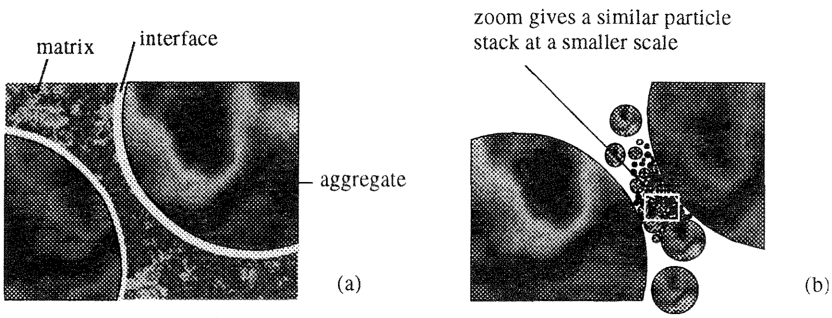

Fig. 2 Concrete regarded as particles 'swimming' in a matrix of cement (a), or as a stack of particles with different size (b), after Van Mier (1997a).

The second approach makes sense when initial microcracking under mechanical load must be explained. In Figure 3a, a stack of regular particles is shown. The particles are loaded uniformly from the top, and depending on the particle contacts, compressive or tensile stress concentrations will appear. Obviously, the weak bonding between aggregate and cement will lead to interfacial cracks as shown in Figure 3b.

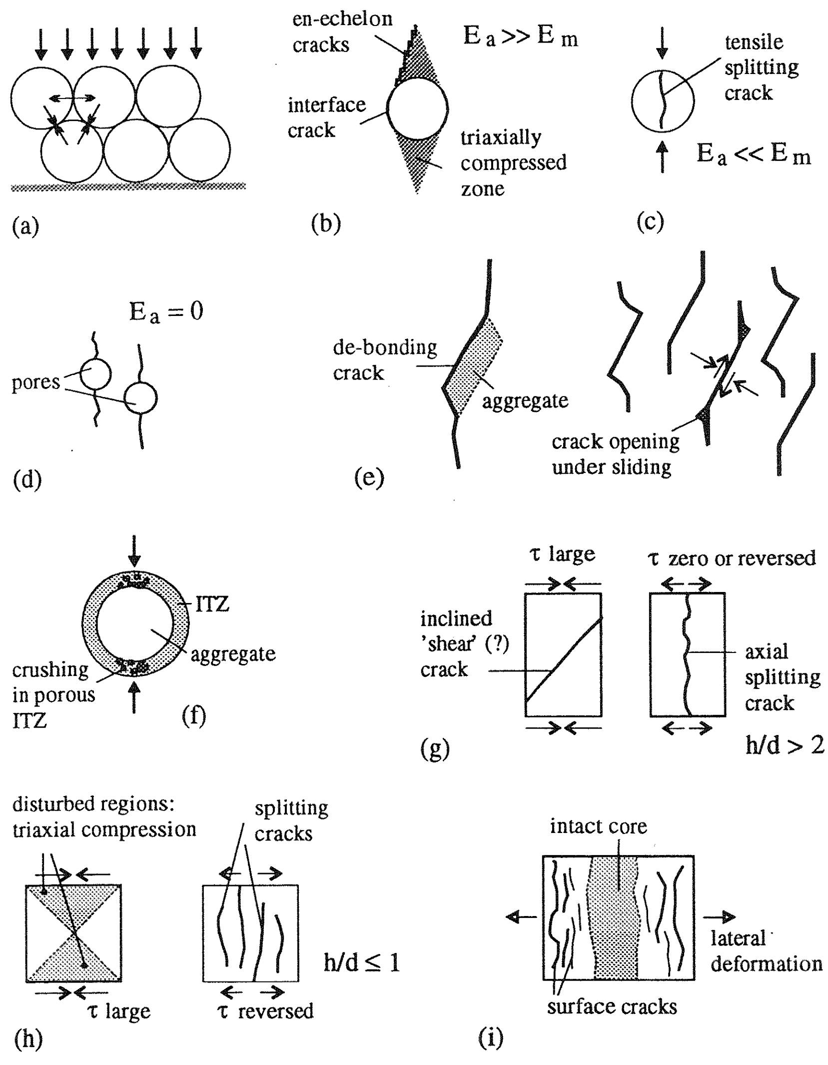

Fig. 3 Different mechanisms for the mechanical behaviour of concrete under uniaxial compression at the meso- and macro-level. The various mechanisms are explained in the text.

The interface cracks may also develop when the model of Figure 2a is considered. The 'soft' matrix will flow around the stiffer aggregates (in normal concrete containing natural aggregates), which may lead to lateral tension and interfacial cracking as shown in Figure 3b. Because the lateral deformations in the relatively soft matrix must be larger than in the stiff aggregates, shear stresses will develop on top and below the aggregates, leading to the well known shear cones that have been reported by many researchers (see also Figure 3b). Failure proceeds through the growth of en-echelon cracks along the sides of the shear cones. The stress state in the shaded shear cones of Figure 3b is triaxial compression, and the matrix will not fail in those regions. The failure mode is however strongly dependent on the stiffness ratio's between matrix and inclusion, where the notion of an inclusion should be extended to porosity (or rather the larger air bubbles). When a lightweight aggregate is used, tensile splitting of the aggregate will prevail as shown in Figure 3c, whereas tensile splitting in the matrix will occur following Figure 3d when stress concentrations around large air inclusions becomes critical. Under high compressive stress (and confined conditions) the pores might eventually collapse. Note that de-bonding cracks may already develop during the hardening stage. Differential temperatures from hydration, differential drying and excessive bleeding water near aggregates may be the cause for the initial cracks. Generally it is considered that vertical cracks in a compressive stress field can propagate only when the global compressive stress is increased. Obviously, the microcracks will never be oriented in a perfectly vertical direction, but rather the growth of wing cracks from initially inclined de-bonding cracks or other imperfections will occur as depicted in Figure 3e.

More recently, a different mechanisms was proposed by Bongers (1998). He proposed that local crushing may occur in the porous interfacial transition zone (Figure 3f). Through this mechanism, large pre-peak deformations could be explained.

The initial Young's modulus of the concrete depends on the stiffness and volumes of the constituting elements in the material. The amounts of aggregate, matrix, interfacial transition zone material and the pore volume determine the value of the concrete Young's modulus, see for example Simeonov & Ahmad (1995a,b), and Van Mier et al. (1998). Through the growth of isolated cracks, the global tangent stiffness of the concrete will gradually decrease. The decrease in stiffness is larger when the number of microcracks increases, or when the individual cracks increase in size.

The various mechanisms mentioned above may not only serve as a crack initiation mechanism, but also they may serve as crack arrestors. For example a crack tip may be blunted when it coalesces with a pore. Such effects will eventually lead to stable pre-peak crack growth processes. Note that the pre-peak non-linear stress-strain behaviour will diminish when the ratio's between aggregate, matrix and interface strength are almost identical, and when the amount and size of the pores is suppressed. These measures would normally lead to concretes with high compressive strength.

The isolated microcracks are generally small enough to ascertain that interactions with the test environment do not occur. Boundary condition and size effects become important around peak stress and beyond peak when the softening regime is reached, and will be treated next.

3 Around peak

When the curvature in the stress-strain diagram increases, and the tangent Young's modulus decreases to zero, the maximum compressive strength of the concrete is reached. The cracks in the material have grown substantially, interactions become important (Figure 3e), and the cracks remain stable only when particular conditions are met. When the test is carried out in load-control, a very brittle collapse will occur, whereas under displacement-control a full softening curve can be measured beyond peak.

Just before the peak is reached, the volume of the specimen will be at a minimum, i.e. the sum of axial and lateral strains will decrease from the origin to a point at approximately 80-90 % of peak stress. After this, the material will dilate, or stated differently, the lateral crack opening has become so large that the specimen volume starts to increase in spite of the large axial compaction. Many researchers in the 1960s and 1970s considered the minimum volume as the onset of global failure of a test specimen. At that stage, cracking has become unstable, and given sufficient amount of time, collapse will be endemic.

Since the size of the cracks and the lateral strains have become large in comparison to the specimen dimensions, boundary conditions and size effects become important, as, for example, can be seen from the results from the RILEM 148SSC committee in Van Mier et al. (1997). For instance, when the slenderness of the specimen is increased in tests between rigid steel loading platens, a decrease of uniaxial compressive strength is observed. The strength approaches an asymptote of 80 % of the cube compressive strength for slenderness larger than 2 to 2.5. In contrast, when low friction boundaries are used such as teflon platens of brushes, the same maximum compressive stress is measured irrespective of the specimen slenderness. Such effects clearly indicate that cracks have reached a critical size near the peak, i.e. critical with respect to the size of the specimen.

4 Post-peak localization

As mentioned, at peak a critical crack length or crack density is reached. After that, the load that can be carried by the specimen decreases when cracks propagate. The stability of the cracked specimen becomes however of extreme importance, and a so-called stable softening curve can only be measured when special experimental procedures are followed. For normal concrete a simple closed-loop test control system using the axial displacement as control variable is sufficient. However, for materials that are extremely brittle such as high strength concrete, additional measures must be taken. Rokugo et al. (1986) proposed an alternative system for test control using a combination of axial load and axial displacement as control variable. Others, like Markeset (1995), use the lateral or circumferential strain as a control variable.

A number of mechanisms is active in the post-peak regime. First of all, unloading occurs in regions that are not cracked because the specimen simply cannot carry larger loads. Secondly, the direction of the macroscopic cracks seems to depend on the amount of boundary shear caused by the loading platens, see Figures 3g,h. Due to boundary restraint triaxially confined regions develop in the parts of the specimen that are in contact with the loading platens. For cubical specimens these disturbed regions represent a considerable part of the specimen (Figure 3h), but for prismatic specimens with $h/d > 2$, generally part of the specimen in not affected, and the concrete can fail along an inclined shear crack (high friction) or through tensile splitting (low friction, see Figure 3g). This was for example shown by Kotsovos (1983), and later confirmed by Vonk (1992). Thirdly, the slope of the descending branch decreases with increasing boundary restraint for specimens of equal size and shape, whereas the rotational freedom of the loading platens plays some role as well, Vonk (1992). It should be noted that for very slender specimens, buckling instabilities may eventually occur, leading to rather un-symmetric modes of failure. In addition to the restraining effects from the loading platens, the slenderness has another important effect on the post-peak curve. This was first demonstrated by Van Mier (1984), and later confirmed by many others, e.g. Vonk (1992), Markeset (1995), Jansen & Shah (1997). In fact, irrespective of the type of loading platen used, localization of deformations occurs in the post-peak regime under uniaxial compression, see van Vliet & Van Mier (1996). This seems to have important implications for analyzing the rotational capacity of reinforced concrete structures, in particular when failure of the compressive zone is decisive, see Hillerborg (1990) and Markeset (1993).

Another important issue is that highly non-uniform deformations occur in the peak and post-peak regimes, see Kotsovos (1983), Van Mier (1984), Vonk (1992) and Choi & Shah (1998). In fact, such measurements seem to indicate that the specimens fail from the outside to the inside, as shown in Figure 3i. An intact core remains, which seems to relate to the post-peak carrying capacity, at least to some extent.

Some researchers (for example Vonk (1992) and Jansen & Shah (1997)) try to determine the fracture energy of concrete in compression. The procedure is similar to the method for determining the fracture energy in tension, but the values are very different indeed. Because the crack density in compression is hard to measure as a direct result from the three-dimensional nature of the fracture process, a direct comparison between tensile and compressive fracture energy is hard to make. One of the complicated factors is of course the structural effect on post-peak compressive and tensile stress-deformation diagrams (geometrical and boundary condition effects such as frictional restraint and the allowable rotations of lading platens are important). It should be noted that quite some frictional energy dissipation is expected to occur in the post-peak regime, whereas large energy jumps are caused from the coalescence of individual cracks as well. The frictional energy dissipation will clearly depend on a number of material parameters, but also on the frictional restraint of the loading platens as argued before.

5 Standard test for uniaxial compression ?

From the work of RILEM TC 148SSC it was found that complete stress-strain curves with relative small scatter can be measured for prismatic specimens (with circular or rectangular cross-section) loaded between teflon loading platens. For a slenderness $h/d = 2$, a narrow scatter band is found, see for example in Van Vliet & Van Mier (1996). The strength of the material approaches the lower asymptote, which is associated with the uniaxial compressive strength, when specimens of this slenderness are used. This implies, that under such conditions, at least a correct uniaxial compression strength is measured, but the post-peak softening curve still depends on the specimen height. When using teflon intermediate layers between the specimen and steel loading platens, an almost unrestrained experiment is carried out. Among others, Vonk (1992) showed that after the well known stick-slip behaviour, teflon has a frictional coefficient below 0.01. Vonk used a single 50 μm thick teflon sheet in combination with Molykote bearing grease between the teflon and the steel loading platen. Van Vliet & Van Mier used a system of two 100 μm thick teflon sheets with a 50 μm thick layer of simple bearing grease in between. A special device was developed to ensure that always the same amount of grease was used. The results showed that the system worked quite well, and it seems a reliable low-friction insert between the steel platen and the concrete specimen. The situation is depicted in Figure 4, and might serve as a future standard test for measuring the complete stress-strain diagram for concrete under uniaxial compression. A cylinder or prism with $h/d = 2$ is loaded between teflon platens as indicated. The specimen should be loaded in a stiff testing machine between a loading platen with a hinge on one side, whereas the other loading platen should be fixed against rotations. The usual demands for compressive testing machines apply, but a closed-loop servo sys-

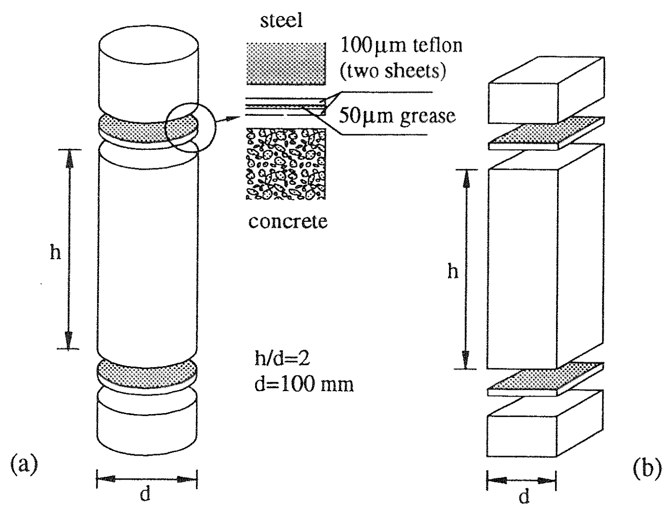

Figure 4 Standard test for determining the complete stress-strain diagram for concrete under uniaxial compression, after Van Mier (1997b).

tem is needed. When high strength concrete is tested, in addition special measures are needed for the control system, e.g. Rokugo et al. (1986). For normal strength concrete, the most optimal feed-back parameter is the total axial deformation of the specimen. It is best measured by means of three LVDTs that are fixed at 120 degrees intervals around the specimen and between the loading platens. It remains to be verified, however, whether the stress-strain diagram measured under such conditions leads to improved and more reliable structural analyses.

6 Impact of compressive softening on structural analysis

Compressive softening is the single most important input parameter in situations where rotational capacity of structures is governed by compressive failure. Different model codes give different stress-strain curves. For example the CEB Model Code 1990 gives a curvi-linear diagram as shown in Figure 5. The relation is a quadratic expression depending on the initial tangent Young's modulus, the strain at peak stress and the peak stress.

$$\sigma_c = -\frac{\frac{E_{ci}}{E_{c1}}\frac{\varepsilon_c}{\varepsilon_{c1}} - \left(\frac{\varepsilon_c}{\varepsilon_{c1}}\right)^2}{1+\left(\frac{E_{ci}}{E_{c1}} - 2\right)\frac{\varepsilon_c}{\varepsilon_{c1}}} f_{cm} \qquad \text{for } |\varepsilon_c| < |\varepsilon_{c,lim}| \tag{1}$$

The various symbols are explained in Figure 5. A fixed value is given for the peak strain, namely ε_{c1} = -0.0022.The descending portion of the stress-strain diagram is valid only for values of $|\sigma_c|/f_{cm} \geq 0.5$. An equation is given to compute the strain $\varepsilon_{c,lim}$ at $\sigma_{c,lim}$ = -0.5 f_{cm}. The slope of the descending branch, in terms of stress and strain, depends on the length of the specimen as mentioned in section 4. In the CEB model code it is mentioned that the above equation is reasonably accurate for a specimen of 200 mm length. In addition to the size effect comes the boundary restraint influence, which has not been considered by CEB. As a consequence, there is reason to investigate whether the current procedures for measuring and handling uniaxial compressive stress-strain curves leads to reliable predictions of structural behaviour.

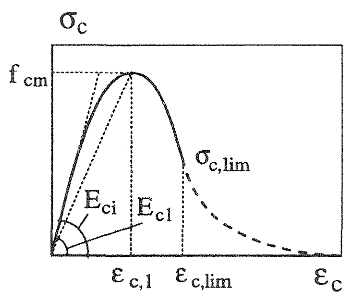

Fig. 5 Stress-strain diagram for uniaxial compression according to the CEB-FIP Model Code 1990.

The simplest case to analyse is a beam subjected to four-point-bending. When sufficient main reinforcement is added with good bond to the concrete, and when sufficient number of stirrups is placed in the support sections to avoid shear failure, compressive failure in the mid-span region is the only remaining mode of failure. At the same time this presents an excellent case to study the effect of parameters related to the pre-peak stress-strain curve and post-peak stress-deformation diagram. The case has been studied experimentally at Aalborg University, and has led to the proposal for a Round Robin analysis by the RILEM technical committee 148SSC "Strain Softening of Concrete" ", see Ulfkjær et al. (1997). The ACI/ASCE Committee 447 on "Finite Element Analysis of Reinforced Concrete Structures participates in the Round Robin. The experimental results have not been released to date, and will be revealed at the workshop II at the FraMCoS-3 conference. The material parameters for the analysis have all been determined, i.e. tensile softening diagrams, compressive softening diagrams between high and low friction loading platens, the steel properties, etc. Of interest is to study the effect of the uniaxial compression diagram, and to investigate whether the proposed new standard test will lead to improved predictions. Sometimes the diagram is modified in a certain model, but the basis, i.e. the measured softening diagram should of course always be as accurate as possible.

7 References

Bongers, H. (1998) Multilevel analysis of concrete in multiaxial compression, **Computational Modelling of Concrete Structures** (eds. R. de Borst, H. Mang, N. Bicanic and G. Meschke), 347-354.

CEB-FIP (1990), **Model Code 90**, Thomas Telford, London.

Chen, W.F. (1982), **Plasticity in Reinforced Concrete**, Mc Graw-Hill.

Choi, S. and Shah, S.P. (1998) Fracture Mechanism in cement-based materials subjected to compression, **J. Engng. Mech. (ASCE)**, 124, 94-102.

Diamond, S. and Huang, J. (1998) The interfacial transition zone: reality or myth ?, in **Pre-Proceedings 2nd Int'l. Conf. on 'The Interfacial Transition Zone in Cementitious Composites'** (eds. A. Katz, A. Bentur, M. Alexander and G. Arliguie), Technion, Israel, 1-40.

Hillerborg, A., Modéer, M. and Petersson, P.-E., (1976) Analysis of crack formation and crack growth in concrete by means of fracture mechanics and finite elements, **Cem. &. Conc. Res**., 6, 773-782.

Hillerborg (1990) Fracture mechanics concepts applied to moment capacity and rotational capacity of reinforced concrete beams, **Eng. Fract. Mech**., 35, 233-240.

Jansen, D. and Shah, S.P. (1997) Effect of length on compressive strain softening of concrete, **J. Engng. Mech. (ASCE)**, 123, 25-35.

Kotsovos, M.D. (1983) Effect of testing techniques on the post-ultimate behaviour of concrete in compression, **Mater. Struct**., 16, 3-12.

Markeset, G. (1993) Failure of concrete under compressive strain gradients, **PhD thesis**, Norges Tekniskes Hogskole, Trondheim, Norway.

Markeset, G. (1997) High strength concrete phase 3E - SP4 - Comments on size dependency and brittleness of HSC, **SINTEF Structures and Concrete**, Trondheim, Norway, February 1995, 23 p.

Mühlhaus, H.-B. (ed.) (1995) **Continuum Models for Materials with Micro-structure**, John Wiley & Sons Ltd., Chichester, UK.

Rokugo, K., Ohno, S. and Koyanagi, W. (1986) Automatical measuring system of load-displacement curves including post-failure region of concrete specimens, in **Fracture Toughness and Fracture Energy of Concrete** (ed. F.H. Wittmann), Elsevier Science Publishers, Amsterdam, 403-412.

Simeonov, P. and Ahmad, S. (1995) Effect of transition zone on the elastic behaviour of cement-based composites, **Cem. Conc. Res**., 25, 165-176.

Simeonov, P. and Ahmad, S. (1995) Interface transition zone and the elastic modulus of cement-based composites, in **Microstructure of Cement-based Systems/Bonding and Interfaces in Cementitious Materials** (eds. S. Diamond et al.), MRS Pittsburgh (PA), 370, 397-406.

Ulfkjær, J.P., Van Mier, J.G.M. and Stang, H. (1997) Invitation to a competition on modelling of over-reinforced concrete beams, **RILEM**

Technical Committee 148SSC "Strain Softening of Concrete" and ACI/ASCE Committee 447 on "Finite Element Analysis of Reinforced Concrete Structures".

Van Mier, J.G.M. (1984) Strain Softening of concrete under multiaxial loading conditions, **PhD thesis**, Eindhoven University of Technology.

Van Mier, J.G.M. (1997a) Fundamental aspects of mechanical behaviour of HS/HPC: The European Approach, in **Proceedings EF Conference on High Strength Concrete** (eds. A. Azizinamini et al.), Kona, Hawaii, (to be published by ASCE New York).

Van Mier, J.G.M. (1997b), **Fracture Processes of Concrete - Assessment of Material Parameters for Fracture Models**, CRC Press, Boca Raton.

Van Mier, J.G.M., Shah, S.P., Arnaud, M., Balayssac, J.P., Bascoul, A., Choi, S., Dasenbrock, D., Ferrara, G., French, C., Gobbi, M.E., Karihaloo, B.L., König, G., Kotsovos, M.D., Labuz, J., Lange-Kornbak, D., Markeset, G., Pavlovic, M.N., Simsch, G., Thienel, K-C., Turatsinze, A., Ulmer, M., Van Geel, H.J.G.M., Van Vliet, M.R.A., Zissopoulos, D. (1997) Strain-Softening of Concrete in Uniaxial Compression - Report of the Round-Robin Test carried out by RILEM TC 148SSC, **Mater. Struct. (RILEM)**, 30(198), 195-209.

Van Mier, J.G.M., Vervuurt, A. and Van Vliet, M.R.A. (1998) Materials engineering of cement-based composites using lattice type models, in **Computational Fracture Mechanics in Concrete Technology** (eds. A. Carpinteri and M.H. Aliabadi), Comp. Mech. Publ., Southampton.

Van Vliet, M.R.A. and Van Mier, J.G.M. (1996) Experimental investigation of concrete fracture under uniaxial compression, **Mech. Coh. Frict. Mater.**, 1, 115-127.

Vonk, R.A. (1992) Softening of concrete loaded in compression, **PhD thesis**, Eindhoven University of Technology.